Journal of the Korean Society of Marine Engineers, Vol.28, No.8, pp.1203~1210, 2004. 11 (ISSN 1226-9549)

Air-Water Two-phase Flow Patterns and Pressure Distributions in a Screw-type Centrifugal Pump

You-Taek Kim†

(Manuscript : Received OCT. 18, 2004 ; Revised NOV. 2, 2004)

Abstract : It was reported recently that the pump head degradation near the best efficiency point from single-phase flow to the break-down due to air entrainment became less in a screw-type centrifugal pump than in a general centrifugal pump. In this paper, I carried out internal pressure measurements and visualizations, and investigated the various physical phenomena occurring inside a screw-type centrifugal pump operated in air-water two-phase flow. The results could give some characteristics about the degradation of pump performance on air-water two-phase flow.

Key words : Two-phase flow, Screw-type centrifugal pump, Pressure distribution, Flow pattern

1. Introduction

A screw-type centrifugal pump is manufactured to carry solids primarily and its impeller has a wide flow passage[1]. The effect of flow passage shape on delay of the break-down due to entrained air and details of characteristics of the pump was investigated by Kim et al.[2] They showed that the screw-type centrifugal pump is more suitable than a general centrifugal pump for transporting air-water two-phase flow because its $\Delta\psi$ (loss of pump head from single-phase flow to the break-down due to air entrainment) near the best efficiency point was smaller. And the effect of flow passage shape on delay of the break-down was little. Moreover, they also reported that the pump head became partially higher in two-phase flow than that in single-phase flow near the best efficiency point at narrow tip clearance. However, the internal pressure fluctuations on this pump due to air entrainment have not been studied yet.

The purpose of this paper is to investigate the relationship between the pump head and the pressure distributions under air-water two-phase flow conditions at n=3,000rpm with different impeller tip clearances, flow coefficients

† Corresponding Author(Dept. of Marine System Engineering, Korea Maritime University)
E-mail: kimyt@hhu.ac.kr

and void fractions by using a small screw-type centrifugal pump designed to acquire basic data. Moreover, the internal flow patterns by using a stroboscope and halogen sheet light was observed. Then, we have investigated the influences of flow patterns on the pressure distributions.

2. Nomenclature

b_2 : width of the volute casing

B_h : height of the blade

C_p : pressure coefficient $(=(P_{imp}-\rho g Z_{imp}-P_s)/(1/2)\rho u_2^2)$

$\overline{C_p}$: mean pressure coefficient during one revolution.

d_{max} : maximum diameter of the impeller

g : acceleration of gravity

H : pump head $(=(P_d-P_s)/(\rho g)+Z_d+(V_d^2-V_s^2)/(2g))$

n : rotational speed

P_d : pressure in the delivery pipe

P_{imp} : pressure measured in the pump casing

P_s : pressure in the suction pipe

Q : volume flow rate of liquid

Q_{gl} : volume flow rate of air

R_{max} : maximum radius of the impeller

T_c : tip clearance

u_2 : peripheral speed at the R_{max}

V_d : mean velocity in the delivery pipe

V_s : mean velocity in the suction pipe

Z_d : height from the pump shaft to pressure tap of P_d

Z_{imp} : height from the pump shaft to pressure tap of P_{imp}

β : void fraction $(=Q_{gl}/(Q+Q_{gl}))$

β_{max} : maximum void fraction

$\Delta\psi$: degradation rate of ψ from single-phase flow to the break-down due to air entrainment $(=\psi_0-\psi_{choke})$

θ_{imp} : phase angle of the impeller

λ : non-dimensional tip clearance $(=T_c/B_h)$

ρ : density of liquid

ϕ : flow coefficient $(=Q/(\pi b_2 d_{max} u_2))$

ψ : head coefficient $(=2gH/u_2^2)$

ψ_0 : head coefficient at $\beta=0$

ψ_{choke} : head coefficient at $\beta=\beta_{max}$

3. Experiment

Schematic view of the small screw-type centrifugal test impeller is shown in Fig. 1. The impeller had 60 degree vertical angle hub corn and had a three-dimensional spiral blade, the maximum radius of which, defined as R_{max}, had a length of 44mm and was located 400 degree from the impeller front tip. The location of R_{max} faced the end of the suction cover casing. The impeller blade width decreased gradually behind R_{max} and vanished at 540 degree. The impeller was made of aluminum. In this paper, tip clearance, T_c, were 0.2mm and 1.0mm. Non-dimensional tip clearances based on the blade height are λ=0.012 and λ=0.058, respectively.

We have set up the experimental apparatus sketched in Fig. 2. Water circulated from a water tank through an electro-magnetic flow meter, a suction pipe, a pump, a flow control valve and a

discharge pipe. The flow rate of liquid was measured by the electro-magnetic flow meter installed in the suction pipe. Air was injected at the location 80mm upstream of the suction cover casing inlet. The water tank had the dimensions of 700mm diameter 600mm height and had a bulkhead at the center. The bulkhead removed air bubbles naturally on the occasion of air-water two-phase flow experiment.

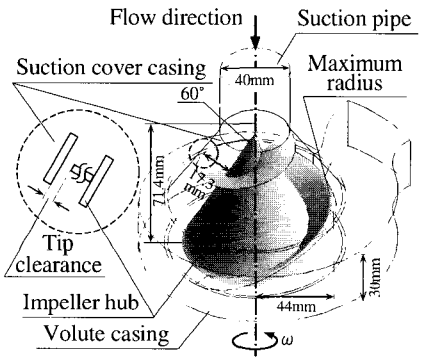

Fig. 1 Test impeller

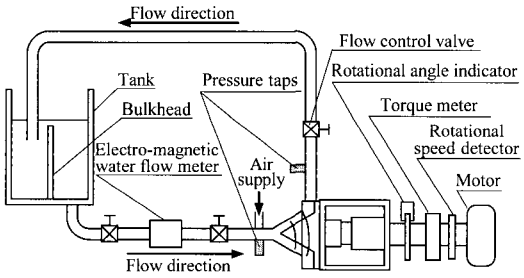

Fig. 2 Schematic view of the experimental apparatus

On the occasion of visualization test, an acrylic-resin-made transparent casing was used. The visualization section is a square of 120mm × 120mm.

The stroboscope was used as a light source to synchronize with the angle of blade. Furthermore, we visualized a rectangle of 80mm × 60mm near the volute tongue by using a halogen sheet light.

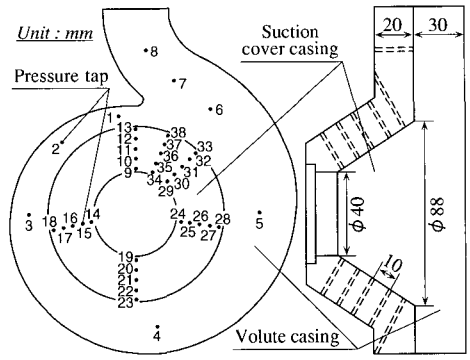

Fig. 3 Locations of pressure taps

Fig. 3 shows the locations of pressure taps on the pump casing which has No. 1~8 measuring holes in the volute casing and No.9~38 ones in the suction cover casing. The volute casing has a rectangular cross section.

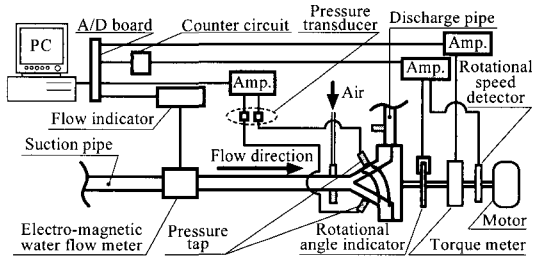

Fig. 4 Measurement system

Fig. 4 shows the measurement system for pressure distributions, which are consisted of semiconductor pressure transducers, amplifiers, an A/D board, and a personal computer. The phase angle of the rotational impeller, θ_{imp}, was measured by a special phase indicator and was defined as 0 degree when the impeller front tip was right vertically

above the pump shaft. A rotational speed detector and a torque meter measured the pump rotational speed and the motor torque, respectively. Pressure fluctuations were evaluated by pressure coefficient, C_p, with averaged ensemble over 100 pump revolutions.

Pressure fluctuation measuring experiment has been achieved mainly at n=3,000rpm, ϕ=0.025 (near the best efficient point).

4. Results and Discussions

Pressure fluctuations during one revolution of the impeller at λ=0.012, β =0 in the different locations, radial (No. 24~28) and peripheral (No. 11,16,21,26) are plotted in Figs. 5(a) and 5(b), respectively. Fig. 5 present that the pressure increases gradually in the radial direction, while there is no increment in the peripheral direction.

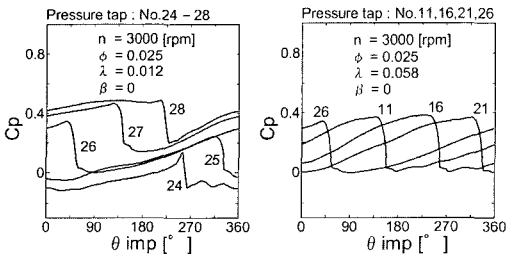

(a) radial (b) peripheral

Fig. 5 Pressure fluctuations in the suction cover casing

Fig. 6(a) and Fig. 6(b) show pressure fluctuations with different void fractions at No. 26 for different tip clearances. In Fig. 6, regardless of λ, the pressure increased with the impeller rotation, dropped right down to the lowest point just after the blade passed and then increased again gradually. However, the width of lowest area is much wider at λ =0.012.

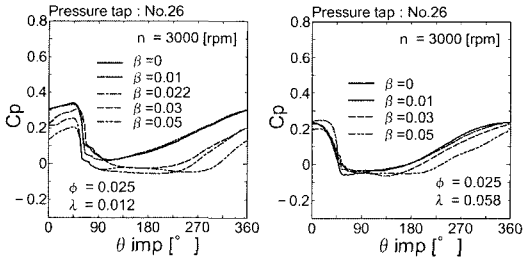

(a) λ=0.012 (b) λ=0.058

Fig. 6 Pressure fluctuations with different void fractions and tip clearances in the suction cover casing

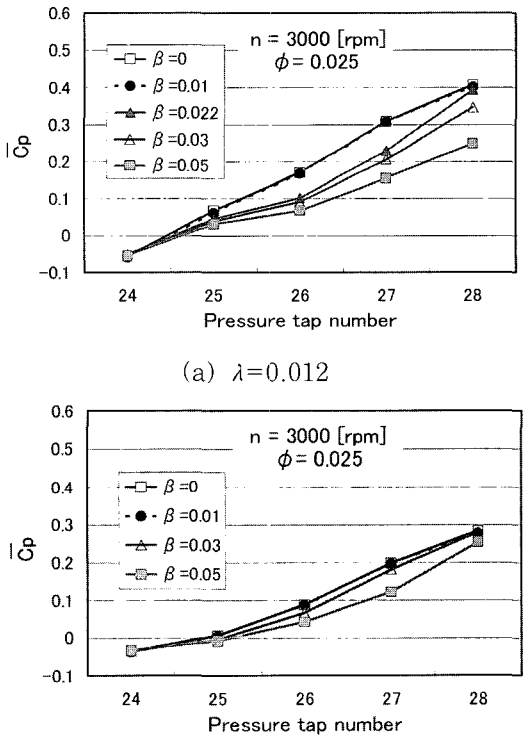

(a) λ=0.012

(a) λ=0.058

Fig. 7 Mean pressure distributions for different tip clearances in the suction cover casing

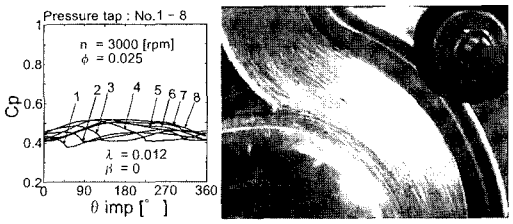

(a) ϕ=0.025

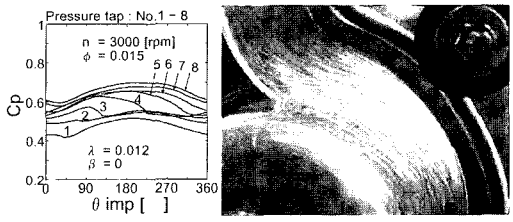

(b) ϕ=0.025

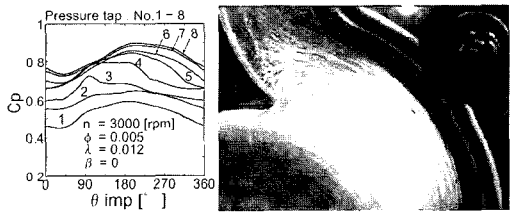

(c) ϕ=0.005

Fig. 8 Pressure fluctuations and flow patterns for different flow coefficients in the volute casing

Mean pressure distributions during one revolution with different void fractions in the radial direction (No. 24~28) at λ =0.012 and λ=0.058 are plotted in Figs. 7(a) and 7(b), respectively. As for β =0.01, pressure distributions are almost the same with β=0 at both tip clearances, while they decrease slowly with the increasing of void fractions at over than β=0.01. When $\overline{C_p}$ at λ=0.012 was compared with that at λ=0.058, the degradation rate of $\overline{C_p}$ becomes less at λ =0.058 than that at λ=0.012. Both tip clearances, $\overline{C_p}$ at β=0.05 has almost the same value for that reason. Consequently, it is considered that the influence of tip clearance on pressure distribution become less, as the void fraction become larger.

Pressure fluctuations at λ=0.012, β=0 with the different flow coefficients, ϕ =0.025, ϕ=0.015, ϕ=0.005 in the volute casing are plotted on the left-hand side of Figs. 8(a), 8(b) and 8(c), respectively. The pictures on the right hand side of those show the flow patterns near the volute tongue of those flow coefficient at β=0.002 taken by using a halogen sheet light. In the volute casing, the peak point of pressure fluctuations appeared once during one revolution, which means the influence of one spiral blade of the impeller appeared intensively in the exit of volute casing. Fig. 8 also show that the growth of pressure gaps between the volute exit (near No. 7, 8) and volute tongue (No. 1) causes gradual increment of recirculating bubbles as the flow coefficient becomes less.

Pressure fluctuations at λ=0.012, β =0.01 with the different flow coefficients, ϕ=0.025, ϕ=0.020, ϕ=0.015, in the volute casing are plotted in Figs. 9(a), 9(b) and 9(c), respectively. In the air-water two-phase flow, as like single-phase flow, the pressure gaps between the volute exit (near No. 7, 8) and volute tongue (No. 1) increase gradually as the flow coefficient becomes less. So, it is considered that the recirculating bubbles increase, as the flow coefficient becomes less.

In order to clarify the influence of recirculating bubbles on pump head

performance, we show the pump head characteristics on n=3,000rpm at λ =0.012 and λ=0.058 in Fig. 10[2]. According to Fig. 10, $\Delta\psi$ near the low flow coefficient was large. Therefore, it is considered that the increment of $\Delta\psi$ near the low flow coefficient was caused by the increment of recirculating bubbles.

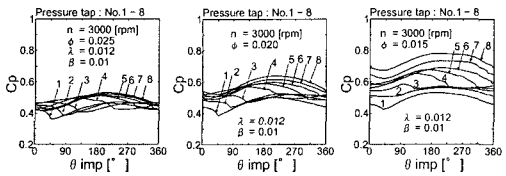

(a) ϕ=0.025 (b) ϕ=0.020 (c) ϕ=0.015

Fig. 9 Pressure fluctuations for different flow coefficients in the volute casing at β=0.01

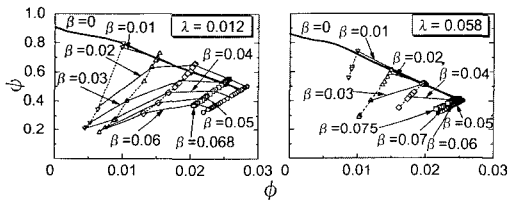

Fig. 10 Screw-type centrifugal pump head characteristics[2]

Mean pressure distributions during one revolution with different void fractions in the volute casing (No. 1~8) at λ=0.012 and λ=0.058 are plotted in Figs. 11(a) and 11(b), respectively. Same with the results in the suction cover casing, the degradation rate of $\overline{C_p}$ becomes less at λ =0.058 than that at λ=0.012. These results coincide well with the change of ψ at ϕ=0.025 in Fig. 10. Moreover, it can be seen that $\overline{C_p}$ at β=0.022 of λ=0.012 becomes higher than that in single-phase flow.

When the results were compared between Fig. 7 and Fig. 11, the increment of $\overline{C_p}$ in suction cover casing was much larger than that in volute casing.

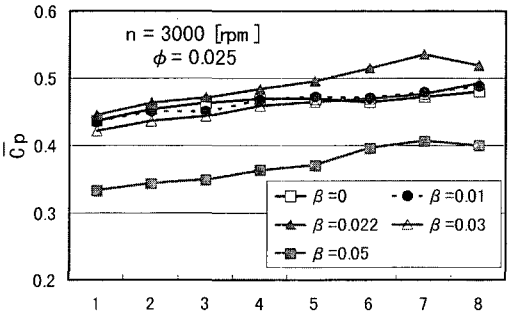

(a) λ=0.012

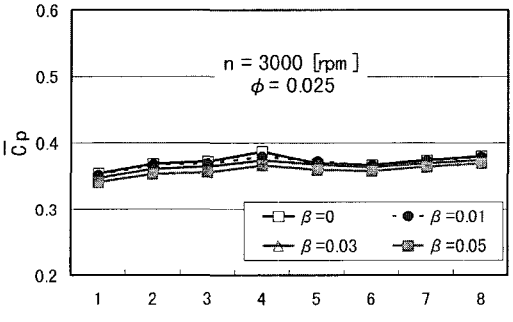

(b) λ=0.058

Fig. 11 Mean pressure distributions for different tip clearances in the volute casing

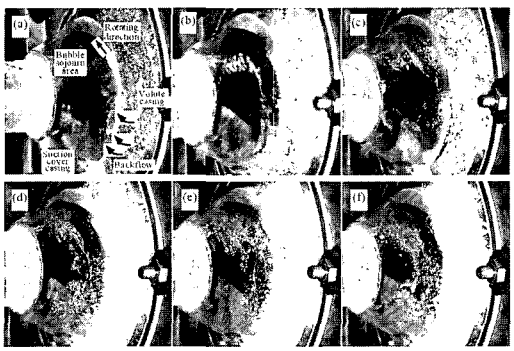

Fig. 12 Flow patterns at n=3,000rpm, ϕ=0.025 and λ=0.012 ;(a) β=0.01, (b) β=0.022, (c) β =0.03, (d) β=0.04, (e) β=0.05, (f) β=0.06

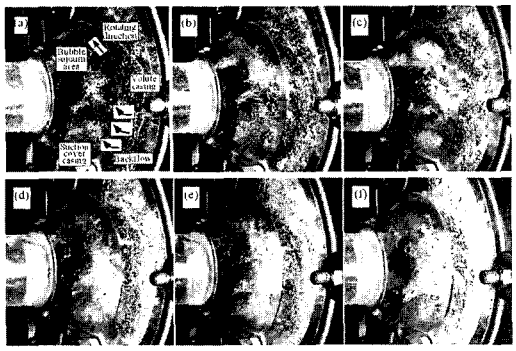

Fig. 13 Flow patterns at n=3,000rpm, ϕ=0.025 and λ=0.058 ;(a) β=0.01, (b) β=0.022, (c) β =0.03, (d) β=0.04, (e) β=0.05, (f) β=0.06

Visualization experiment by using a stroboscope has been achieved under the conditions of n=3,000rpm and ϕ=0.025. Fig. 12 and Fig. 13 show the flow patterns at λ=0.012 and λ=0.058, respectively. The impeller rotates from the bottom to the top. The rear side of blade is pressure surface and the front side of one is suction surface. These pictures show that the transition of bubble sojourn area formed suction surface of the impeller blade. In this screw-type centrifugal pump, bubbles stay always in the suction surface of the blade, regardless of void fractions and tip clearances. However, the sojourn area remains as large lumps of bubbles at λ =0.012, while it does with dispersion by much of leakage flow at λ=0.058. So, it is considered that the increment of lowest area of $\overline{C_p}$, after the blade passed at λ =0.012 as shown in Fig. 6(a), is due to large lumps of bubbles in the suction surface. This causes much degradation of ψ at λ=0.012, as shown in Fig. 10.

Near the exit of suction cover casing, large-scale backflow occurs always because of the secondary flow in a screw-type centrifugal pump. Large-scale backflow, from volute casing to suction cover casing, can be seen at all Fig. 12 and Fig. 13 except Fig. 12(b). Fig. 12(b) shows well-fixed air band, which was formed at the suction surface of the blade to the end of suction cover casing, blocked the backflow. It explains sufficiently the result that $\overline{C_p}$ at β =0.022 of λ=0.012 became higher than in single-phase flow. The other cases, the bubble sojourn area in the suction surface were crashed and dispersed by much of leakage flow, and air band could not be formed. Therefore, pump head increment can not be seen in these cases because there is no air band to block the backflow.

4. Conclusions

We carried out the pressure fluctuation measurement and visualization experiments under air-water two-phase flow conditions at n=3,000rpm with different impeller tip clearances, flow coefficients and void fractions by using the small screw-type centrifugal pump designed to acquire basic data.

(1) The influence of tip clearance on pressure distribution becomes less, as the void fraction becomes larger.

(2) The increment of pump head degradation rate near the low flow coefficient is caused by increment of recirculating bubbles.

(3) Both in the suction cover casing and in the volute casing, the degradation rate of pressure distribution becomes less at

wider tip clearance. These results coincide well with the change of pump head.

(4) The pressure increment in suction cover casing is much larger than that in volute casing.

(5) Pump head degradation rate mainly depends on the dimensions of bubble sojourn area formed suction surface of the impeller blade.

(6) Peculiar phenomenon that the pump head became partially higher in two-phase flow than that in single-phase flow is due to pressure increment in the volute casing.

References

[1] Tanaka, K., and Matsumoto, Y., 1988, "Experimental Study of Radial Thrust on Screw Centrifugal Impeller," Annual Report of Engineering Research Institute, Faculty of Engineering, The University of Tokyo, pp.185-192.

[2] Kim, Y.T., Tanaka, K., and Matsumoto, Y., 1999, "Tip Clearance and Bubble Size of a Screw-type Centrifugal Pump Operating in Two-phase Flow," Proceedings of the 3rd ASME/JSME Joint Fluids Engineering Conference, FEDSM99- 7207.

Author Profile

You-Taek Kim

He received his B.E. and M.Eng. degrees from Korea Maritime University, and his Dr.Eng. from Kyushu Institute of Technology, Japan. He is currently an assistant professor in the Dept. of Marine System Engineering at Korea Maritime University in Busan, Korea. His research interests include fluid machinery, two-phase flow, cavitation, CFD.